Zeitschrift: Helvetica Physica Acta
Band: 53 (1980)
Heft: 1

Artikel: Magnetoacoustic oscillations in a plasma produced by radiofrequency discharge

Autor: Schneider, H. / Hoegger, B.A. / Ritz, Ch.

DOI: https://doi.org/10.5169/seals-115108

Nutzungsbedingungen
Die ETH-Bibliothek ist die Anbieterin der digitalisierten Zeitschriften. Sie besitzt keine Urheberrechte an den Zeitschriften und ist nicht verantwortlich für deren Inhalte. Die Rechte liegen in der Regel bei den Herausgebern beziehungsweise den externen Rechteinhabern. Siehe Rechtliche Hinweise.

Conditions d'utilisation
L'ETH Library est le fournisseur des revues numérisées. Elle ne détient aucun droit d'auteur sur les revues et n'est pas responsable de leur contenu. En règle générale, les droits sont détenus par les éditeurs ou les détenteurs de droits externes. Voir Informations légales.

Terms of use
The ETH Library is the provider of the digitised journals. It does not own any copyrights to the journals and is not responsible for their content. The rights usually lie with the publishers or the external rights holders. See Legal notice.

Download PDF: 04.10.2024

ETH-Bibliothek Zürich, E-Periodica, https://www.e-periodica.ch

Helvetica Physica Acta, Vol. 53 (1980), Birkhäuser Verlag, Basel

Magnetoacoustic oscillations in a plasma produced by radiofrequency discharge*

by **H. Schneider, B. A. Hoegger, Ch. Ritz, B. G.Vaucher** and **T. M. Tran**†

Department of Physics, University of Fribourg, Fribourg/Switzerland

(13. II. 1980)

Abstract. Magnetoacoustic oscillations in a Helium plasma are investigated. The plasma is strongly inhomogeneous. The average density is $n_e \approx 4 \cdot 10^{12}$ cm^{-3}, but drops to an immeasurable value near the wall. The device, in which an r-f-discharge produces this profile, is described.

The results of a theoretical calculation are given. This calculation is based on a three fluid cold plasma theory and the density and temperature profile as well as the finite length of the plasma column and the length of the exciting coil is taken into account. It is shown that the experiments can only be described by this calculation, if an effective collision rate is introduced. This ν_{eff} might be justified by observed fluctuations at the boundary of the plasma.

I. Introduction

In magnetoacoustic oscillations the oscillating masses are the ions and electrons in the plasma and the restoring force is the magnetic pressure as described by the Maxwellian stress tensor. This phenomenon has attracted much interest in recent years, because these waves transport considerable energy and – as Alfvén [1] has shown – might play a role in space as well as in the interior of stars.

Beside this very general interest in this field different authors [2–5] have proposed or tried to use these waves in fusion devices to heat the plasma. The advantage is evident since these devices work with strong magnetic fields and relatively low frequencies can be used where oscillators with high power are available.

Heating of course presumes that there is a mechanism providing strong dissipation. So the demand is, that the wave should penetrate easily into the plasma and is absorbed in the plasma and not in the boundary or even being reflected. This demand can be met if a geometric resonance is excited.

In collision dominated plasmas (e.g. $n_e \approx 10^{15}$ cm^{-3} and $T_e \approx 2$ eV), where the mechanism of dissipation is well known (Ohmic) a considerable amount of energy is dissipated in the plasma [6] and the resonances have been studied in detail [7]. However, the plasmas in space are so diluted, that they rather must be regarded

* Supported by the Swiss National Science Foundation

† Present address: Laboratoire de Génie atomique, Swiss Federal Institute of Technology, Lausanne/Switzerland

as collisionless and the fusion device is expected to work at such high temperature that this situation also must be regarded as collisionless.

The question now arises, what is the dissipation of these waves if the classical collisions are no longer responsible for the damping of the geometric resonances. The answer to this question must be found in experiments with high temperature or low density. But geometric resonances depend also on the size of the plasma and the available magnetic field and practical considerations of coupling the radiofrequency to the cylinder, and other limitations. For these reasons our experiments are performed at a density of $n_e \sim 10^{12}\,\mathrm{cm}^{-3}$ and here – since collisions still play a role – the interpretation of the results becomes intricate. Not only the collisions have to be considered but also the finite size of the plasma cylinder and the inhomogeneity of the plasma. Perhaps still other mechanisms have to be taken into account [9] and finally nonlinear effects have to be studied.

Here we are dealing only with linear effects and the influence of the inhomogeneity produced by the microwave discharge on the magnetoacoustic field distribution.

II. The apparatus

Plasmaproduction. The plasma is produced in a pyrex tube of 9.2 cm inner diameter and 100 cm length. The device (MOLESON) is shown schematically in Fig. 1. The background pressure measured by a Bayard Alpert gauge is below 10^{-6} Torr. In the discharge region the gas pressure is monitored by a Barocell capacitive pressure gauge in the range of $10^{-4} - 10^{-2}$ Torr.

A direct current magnetic field in axial direction is excited by twenty water cooled coils. The spacing of these coils is adjusted to produce a homogeneous field ($\Delta B/B \leqslant 1\%$) of up to 2500 Gauss in the main part of the tube. On one side the spacing is increased. Here the magnetic field decreases and reaches the electron cyclotron resonance condition for the given frequency of the preionization microwave structure.

The plasma production occurs in two steps by identical microwave guns in pulses of 1 ms length and a repetition frequency of 50 Hz. So all observations are made 50 times per second either during the production period of plasma or in the afterglow. Since the decay time is in the order of milliseconds transient as well as stationary effects can be observed. The slow wave structure consists of six windings with inner diameter of 10 cm and a pitch of 1 cm and the microwave power is fed to the helix by a coaxial structure tapped to the centre of the windings.

The initial plasma, which is necessary for the anomalous absorption of intense microwave power at high magnetic fields – as was shown by J. Musil and F. Zacek [10] – is produced at electron cyclotron resonance (8 in Fig. 1). This preionization plasma fills the total length of the tube. The main discharge is provoked in the high field region by two microwave guns which act on the background plasma.

Figure 2 shows the scheme of the main microwave power system. A CW magnetron with a nominal output of 6 kW at 2.45 GHz is used. At the output of the magnetron a three port wave guide circulator suppresses reflections of microwaves from the plasma which would shift the frequency and the level of the

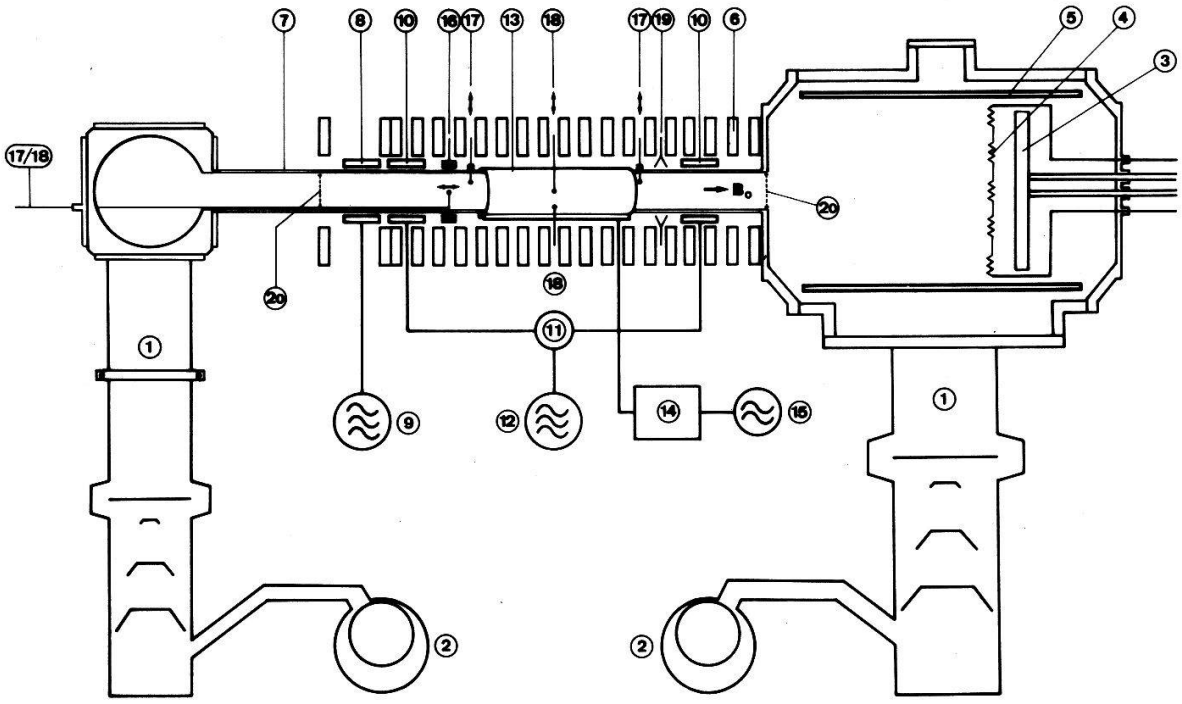

Figure 1
Experimental apparatus. 1. oil diffusion pumps 2500 1/s, 2000 1/s; 2. backing pump; 3. anode; 4. filament cathode; 5. dipole magnets; 6. magnetic field coil; 7. pyrex glass tube; 8. microwave structure-preionization; 9. microwave generator; 10. mw-structure – main discharge; 11. power divider; 12. mw-power generator; 13. single turn coil-magnetoacoustic-wave structure; 14. impedance matching network with directional coupler (Merrimac type CR-30-15, 1-30 MHz); 15. *rf*-sine wave generator and broadband amplifier (ENI-3100 L, 0.1-100 MHz, 100 watts PEP); 16. diagnostic coil system; 17./18. radial and axial probes; 19.8 mm mw-interferometer; 20. grids for axial plasma limit. The hot cathode assembly (3, 4, 5) is foreseen for low density steady state experiments.

generator. Subsequently the power is divided into two parts by a hybrid ring as described by M. A. Heald and C. B. Wharton [11]. Wave guide to coaxial transitions are necessary to bring the high frequency with cables to the helical structure. The matching is performed with a three stub tuner. The incident and the reflected power is measured by means of a calibrated dual broadband coaxial directional coupler.

The magnetron is powered by a pulsed d.c. supply. Ten high voltage transistors simultaneously switched by optically decoupled circuits deliver the pulses (7.7 kV, 1.6 A) of variable duration (0.1–2.5 ms). The generator is triggered with a delay of 200 μs with respect to the ignition of the preionization.

Plasma excitation. The radiofrequency for the magnetoacoustic experiments is generated with a gated sinewave generator in connection with a broadband amplifier to bring the desired signal to a level of $\leqslant 3$ watts (15 in Fig. 1). The gate pulse is synchronized to the microwave discharge with delay lines. Hence the delay and the length of the burst can be choosen. An impedance transforming network couples the radiofrequency to a single turn coil around the discharge tube. Incident and reflected power is measured with a directional coupler. This antenna (44 cm long) can be matched with a standing wave ratio (SWR) to better than 1.2 to the impedance of the amplifier.

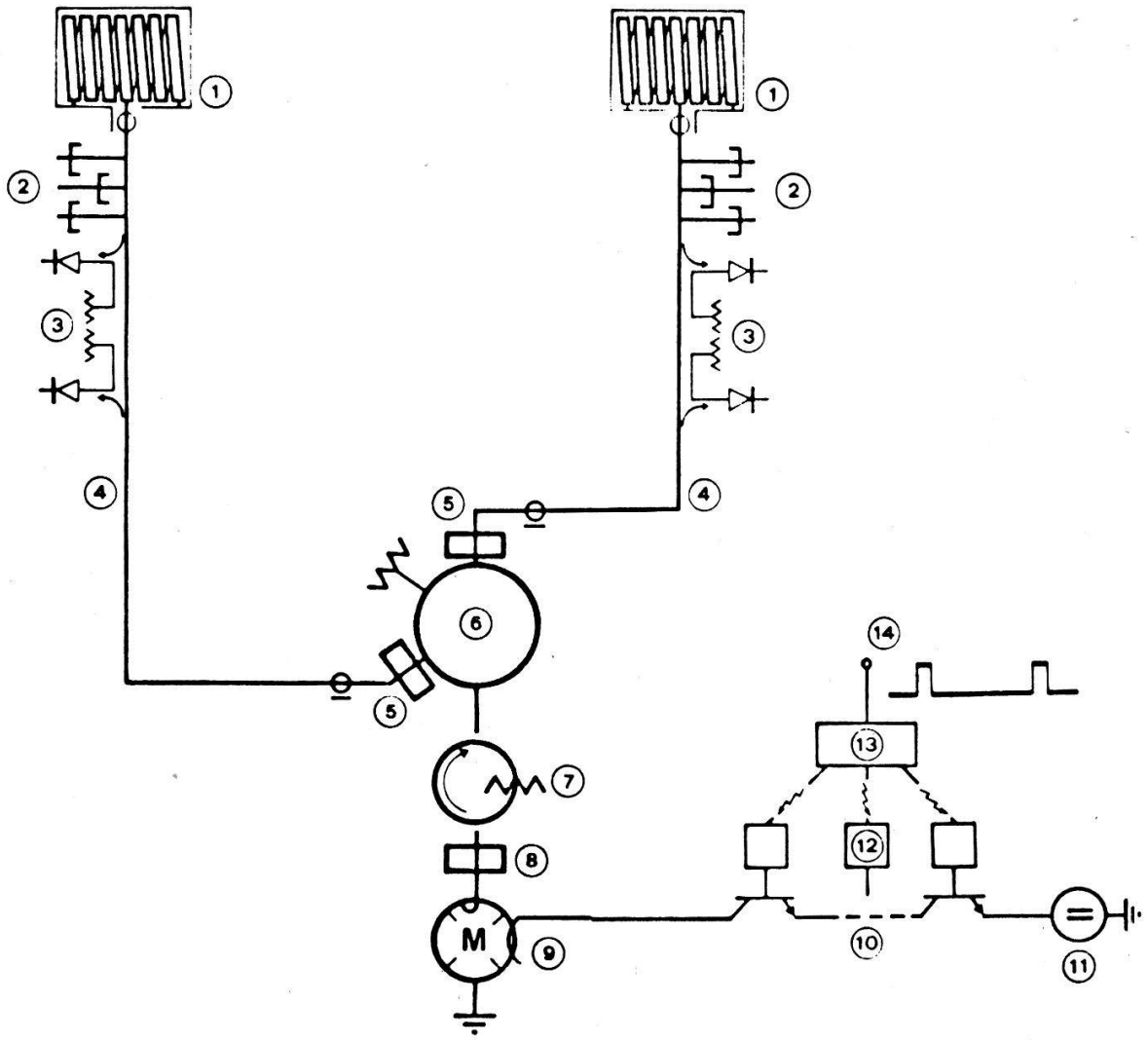

Figure 2
Microwave system. 1. slow wave structure; 2. triple stub tuner; 3. dual broadband directional coupler (Rhode & Schwarz type ZDF); 4. coaxial cable (Suhner type RG 220/U); 5. waveguide to coaxial transition; 6. powerdivider-hybrid ring; 7. waveguide circulator; 8. magnetron rf-coupling structure; 9. magnetron (Philips type YJ 1191); 10. high voltage switching cascade (Philips type BU208 transistors); 11. dc-power supply; 12. transistor switching units; 13. optocoupler (Optron type OPI 113); 14. pulse shaping network.

Diagnostic methods. The mean plasma density is measured with an 8 mm microwave interferometer.

Cylindrical Langmuir and double probes and wavelaunching grids can be shifted along the z-axis and at six different positions in radial direction. The radial and axial position of the probes is monitored on the x-axis of an x-y-recorder. Figure 3 shows the diagnostic system. The radial density profile is measured with floating double probe in the ion-saturation mode. A new optically decoupled circuit [12] and dc/dc converter technique is applied to suppress the common mode due to large potential variation observed in these pulsed inhomogeneous plasmas. The temperature is obtained from the voltage-current characteristic.

Magnetic probes – moveable in radial and axial direction – measure the distribution of the excited radiofrequency field. The rf signal from the probe passes a

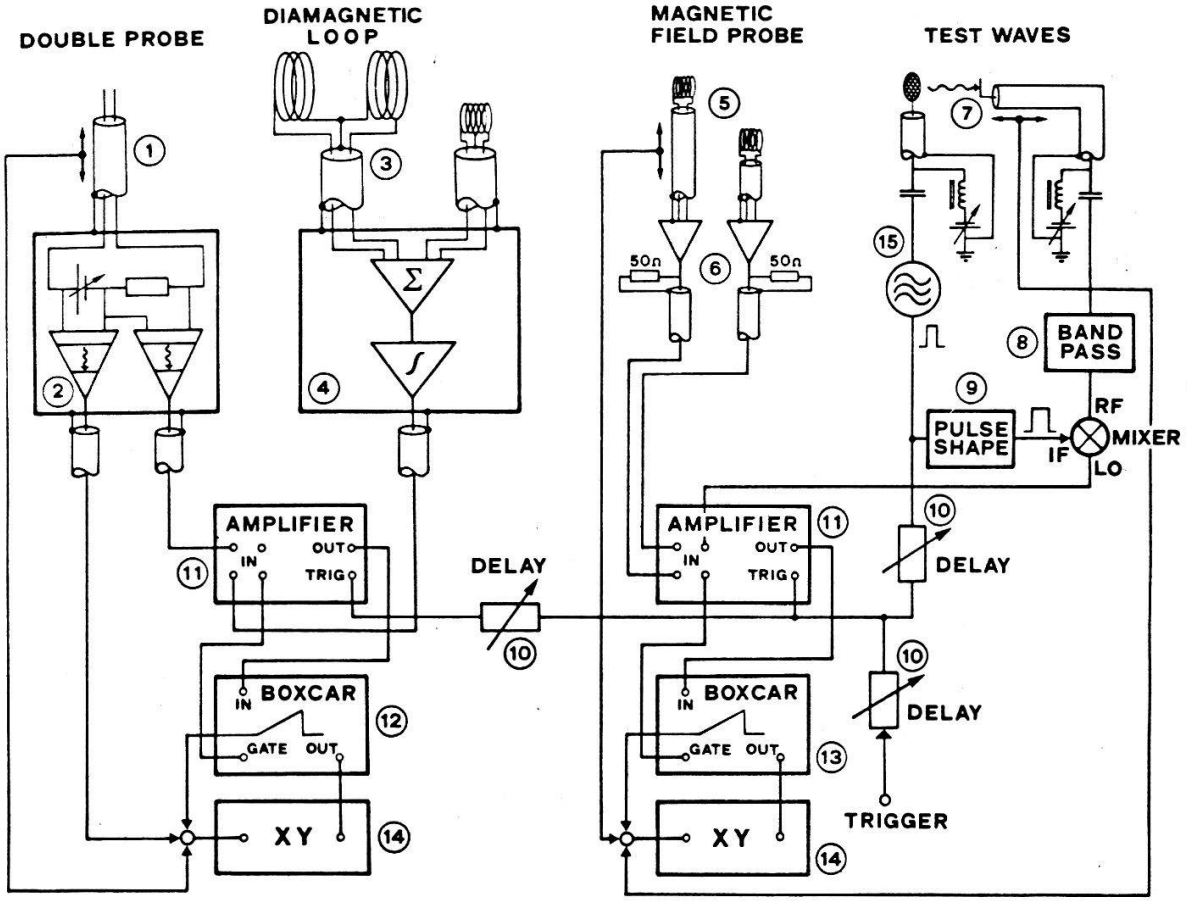

Figure 3
Diagnostics. 1. floating double probe; 2. probe current and voltage sensing amplifier with optocoupler system; 3. diamagnetic loop; 4. compensation and integration amplifier; 5. magnetic field probe; 6. preamplifier; 7. test wave grid and cylinder probe; 8. band pass amplifier; 9. pulse shape circuit; 10. delay line; 11. c.r.t.-amplifier; 12. and 13. BOXCAR-averager; 14. X-Y recorder.

broadband impedance matching amplifier and all signals of the diagnostic are recorded in a Faraday cage.

A diamagnetic coil technique is used to measure the energy content of the plasma. This coil (100 windings) has a central tap and works in differential mode to suppress signals due to direct pickup. An additional compensation coil was necessary to compensate for low frequency fluctuations of the magnetic field.

Sampling technique is applied in all these diagnostic methods except the microwave interferometer. All results are plotted directly on the x-y-recorder. The requirements to the triggering accuracy is considerable and high precision delay lines are used. The sampling is performed by box cars. Two types of box cars are in use, a PAR 162 and a TEKELEK 9870. Simultaneous measurements are possible.

III. Physical model

A computer code REGINA [13] has been written to calculate the field distribution in a magnetized plasma cylinder excited by a concentric coil. The procedure is similar to that used by other authors [15, 7] but radial density and temperature profiles can be taken into account.

We consider a three fluid plasma, immersed in a uniform axial magnetic field. The pressure terms are neglected but collisions between ions and electrons and neutrals and ions with neutrals are considered. The total collision frequency can be enhanced to introduce even radial dependent effective collision frequencies [14] when the strong damping of the magnetoacoustic resonance cannot be explained by cold plasma theory. The components of the dielectric tensor are easily obtained from the fluid equations. To take into account the finite length of the plasma cylinder we assume perfectly conducting end walls.

Therefore the calculation can be based on Fourier expansion in terms of $k_z = m\pi/L$, where L is the plasma length and m is an integer.

Method. The discretization of the linearized Maxwell equations is made by means of a finite difference scheme. Outside the plasma the problem is solved treating the excitation coil as an azimuthal current sheet. Using the resulting boundary conditions the algebraic system is solved by Gaussian elimination with search for pivots. We found that for our profiles considering 41 points on the r-grid and 31 Fourier components was sufficient.

The actual version of the code yields the oscillating magnetic field $B_z(r)$ at an axial position z and its phase shift over the plasma radius as a function of the applied frequency. The B_z component is normalized by its value outside the plasma cylinder.

Numerical results. The oscillating magnetic field $B_z(r, z; \omega)$ is calculated for different density and temperature profiles to demonstrate the influence of an inhomogeneity in the plasma. Figure 4 shows three assumed profiles with equal

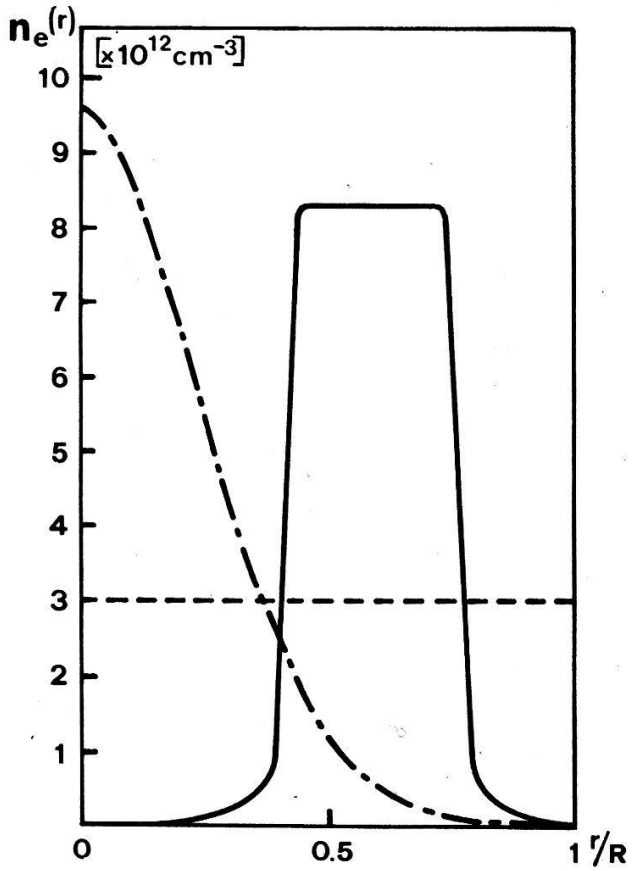

Figure 4
The assumed electron density profiles.

average density: a homogeneous plasma, a Gaussian density distribution and a hollow plasma cylinder. The temperature is assumed to be constant over the radius. The plasma parameters are in the range of the experiments reported in this paper. The computed oscillating field and its phase shift as a function of frequency are shown in Fig. 5. For each density profile the first magnetoacoustic

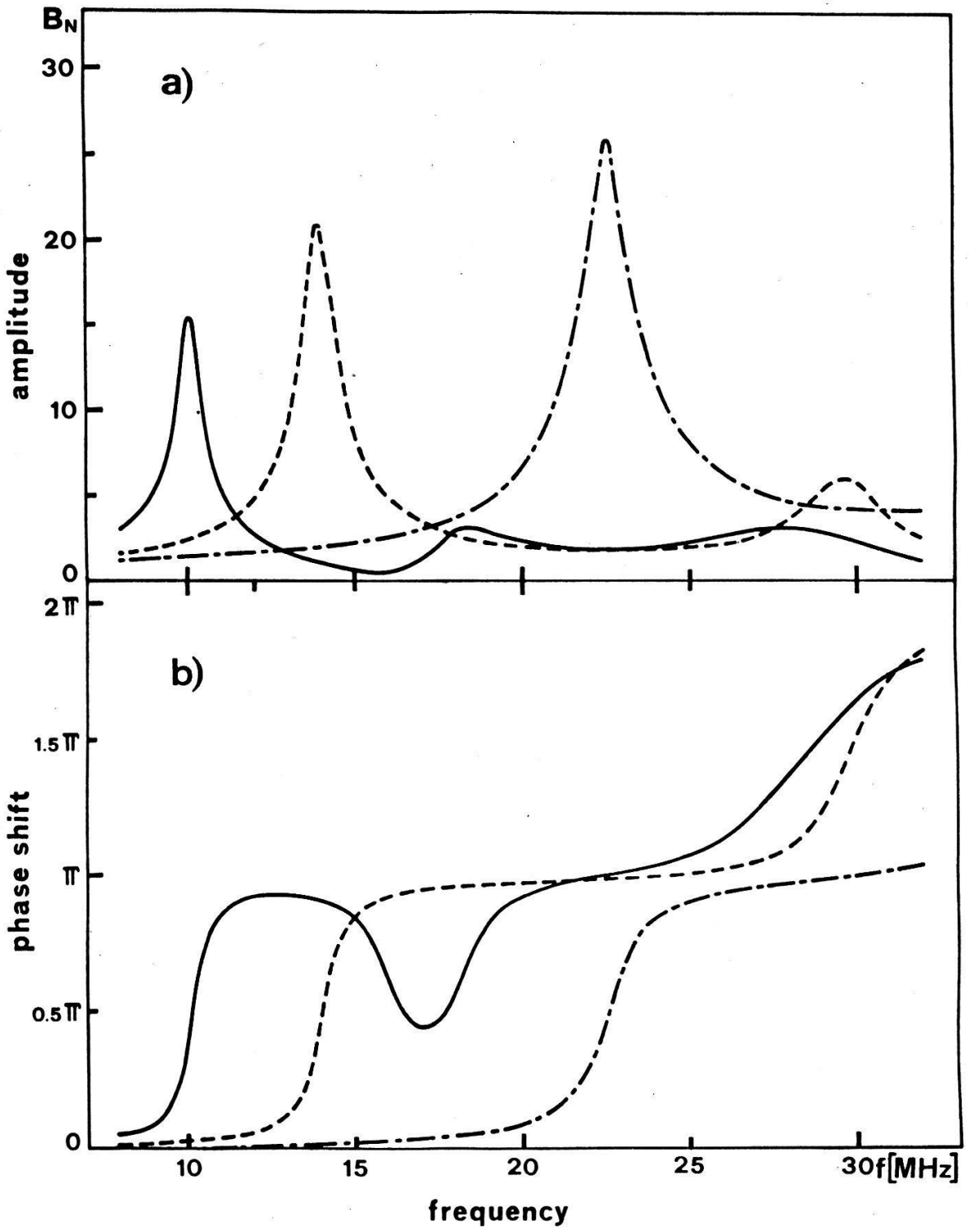

Figure 5
Normalized magnetic field. $B_N = B_z(r=0, z=L/2)/B_z(r=R, z=L/2)$ and its phase shift $\Delta\phi = |\phi(0)-\phi(R)|$ as a function of frequency. Dashed, dotted and solid line refer to the respective density profiles in Fig. 4. Helium gaz, $P_O = 10$ mTorr, $T_e = 4$ eV, $T_i = 0.1$ eV, $\langle n_e \rangle = 3 \cdot 10^{12}$ cm^{-3}, $B_o =$ 2 kG, $L = 80$ cm, plasma radius 4.6 cm, coil length 40 cm.

resonance can be identified. At this resonance frequency the phase shift is $\pi/2$. The amplitude is only slightly affected by a strong inhomogeneity in the density. With pure frictional damping considered in this calculation the field amplification is at least fifteen. The resonance frequency is drastically shifted. This can be qualitatively understood considering an effective plasma radius given by the assumed density profiles.

The shape of the radial profile of the magnetic field is also strongly affected. Figure 6 shows the radial profiles of B_z for the assumed density distributions. The homogeneous plasma yields the typical field distribution of the first magnetoacoustic resonance. In a hollow plasma cylinder the field enhancement takes place only in the plasma region and the field amplitude remains constant in the inner plasma free region. For a Gaussian density distribution the field profile is similar to a Gaussian.

Figure 7 shows three assumed temperature profiles with equal average temperature. The electron density is assumed to be homogeneous over the radius. In Fig. 8 is shown how the radial field profile B_z is modified by the inhomogeneity in the temperature. The plasma parameters are the same as above. If the electron temperature increases quadratically to the plasma edge the radial field profile is almost the same as in the homogeneous case. The Gaussian temperature distribution however with the dominant outer region filled with cold plasma yields a drastic damping and frequency shift of the first magnetoacoustic resonance.

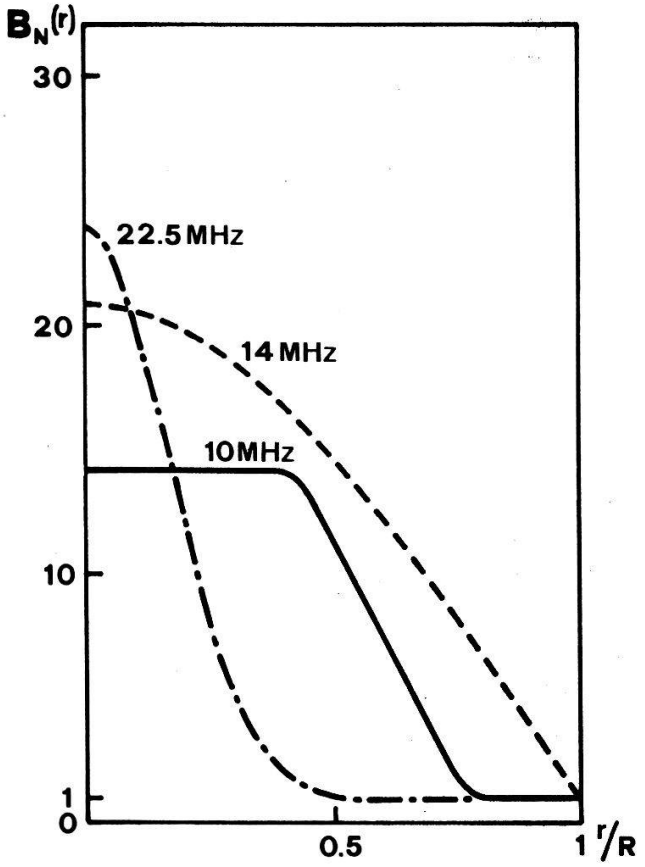

Figure 6
Normalized $B_N(r, z = L/2)$ computed at the first magnetoacoustic resonance frequency. Dashed, dotted and solid line refer to the respective density profiles in Fig. 4. Plasma parameters as in Fig. 5.

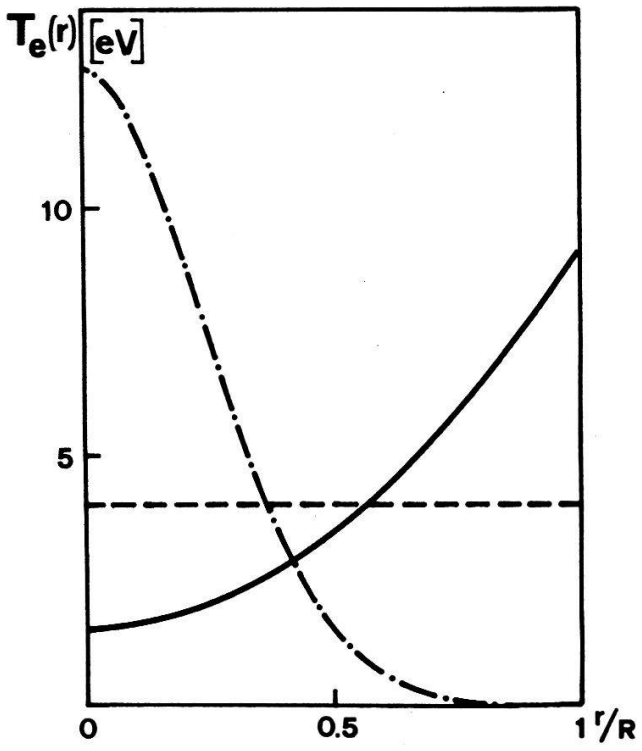

Figure 7
The assumed electron temperature profiles.

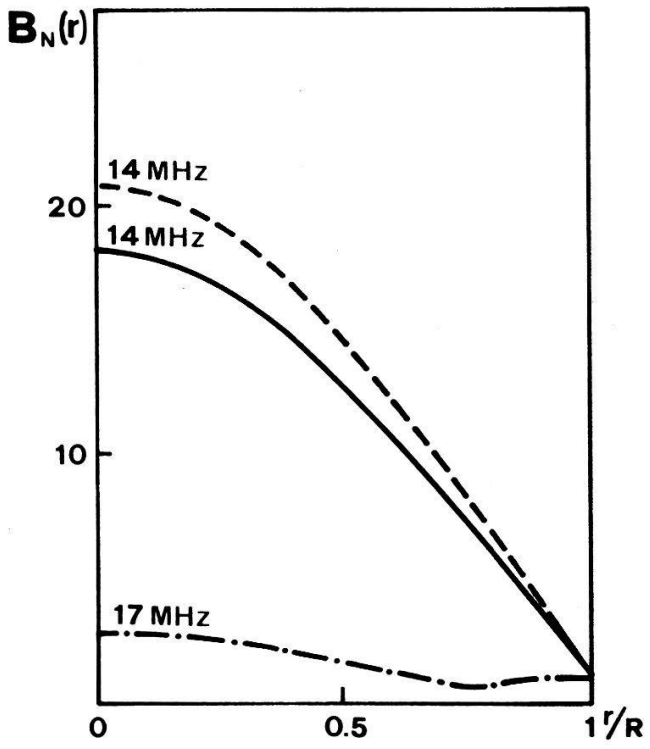

Figure 8
Normalized ($B_N(r, z = L/2)$ computed at the first magnetoacoustic resonance frequency. The dashed, dotted and solid line fefer to the respective temperature profiles in Fig. 7. Plasma parameters as in Fig. 5.

IV. Experimental results

The most important observation in all experiments with Helium at this density is, that the amplitudes of the geometric resonances are very small. To demonstrate the discrepancy between experiments and theory we show in Fig. 9 the measured and calculated amplitude in logarithmic scale. The first peak at 12 MHz is the first resonance in radial direction. This assignment is supported by phaseshift and radial distribution (see Fig. 11 and Fig. 12).

The two other peaks at 25 MHz and 29 MHz are assigned to axial modes. The two corresponding maxima are also given by theory but at lower frequency. This is easily explained by the fact, that axial modes are strongly affected by the length L of the cylinder and possibly the effective length of the column is slightly smaller than the distance between the two grids in the discharge tube.

The remarkable fact is that the theory gives an amplitude amplification of about 20 for the first radial resonance whereas in the experiment only a factor of 2–3 is found. This is far out of any experimental error and can no longer be explained by inhomogeneity since the measured density and temperature profile has been considered in our calculation. Moreover it was shown in our numerical calculation (see Fig. 4 and Fig. 6) that even an extreme inhomogeneity in the

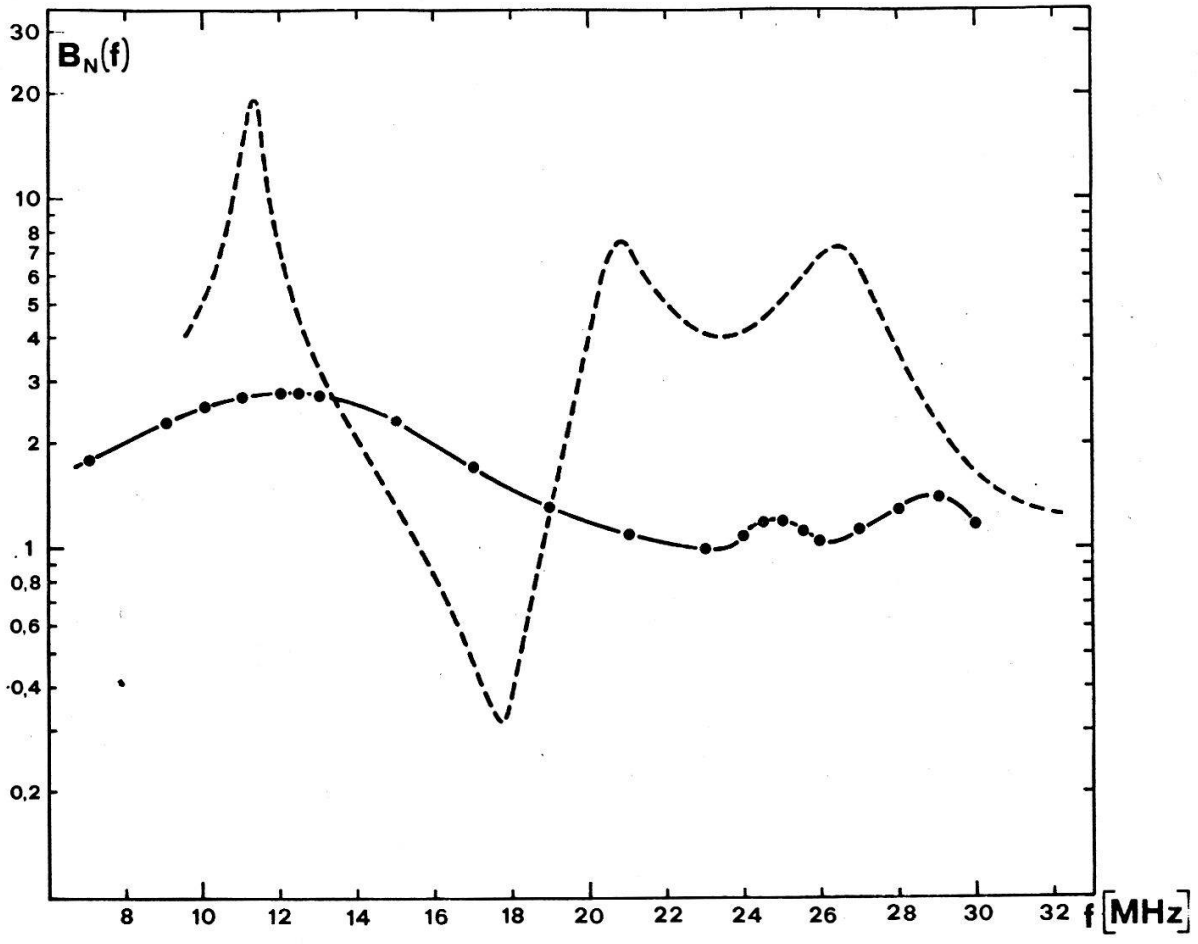

Figure 9
Magnetoacoustic resonances in logarithmic scale. Dots represent experiments. Dashed line is the result of the numerical calculation.

density cannot produce such a damping. The radial dependence of the electron temperature was measured and found to be constant within experimental errors ($T_e = 4.0 \pm 0.1$ eV).

The density profile used to calculate the theoretical amplitude in Fig. 9 is shown in Fig. 10. The density has a minimum on the axis. This is a general quality of plasma produced by slow wave structures and has been observed by other authors [10]. Moreover we observe fluctuations which seemingly are most pronounced at the steep decrease of the density at the boundary. The spectrum of these fluctuations has been analysed with a spectrum analyser and appears to be fairly constant between 0.05 MHz and 2 MHz. No pronounced peaks are observed, but the amplitude of the fluctuations strongly depends on the radius.

An auto-power-spectrum of the fluctuations at 100 kHz (bandwidth 30 kHz) has been recorded. The radial dependence of this signal is shown in Fig. 10(b). Note that no absolute value is obtained in this way. But the increase of this signal by 35 dB means that the amplitude of the fluctuations is increased by a factor of 50. Similar observations have been made in a stellarator by Vojtsenya et al. [16].

It suggests itself that this enormous increase of fluctuation energy has an effect on the resistivity. We have therefore introduced an enhancement of

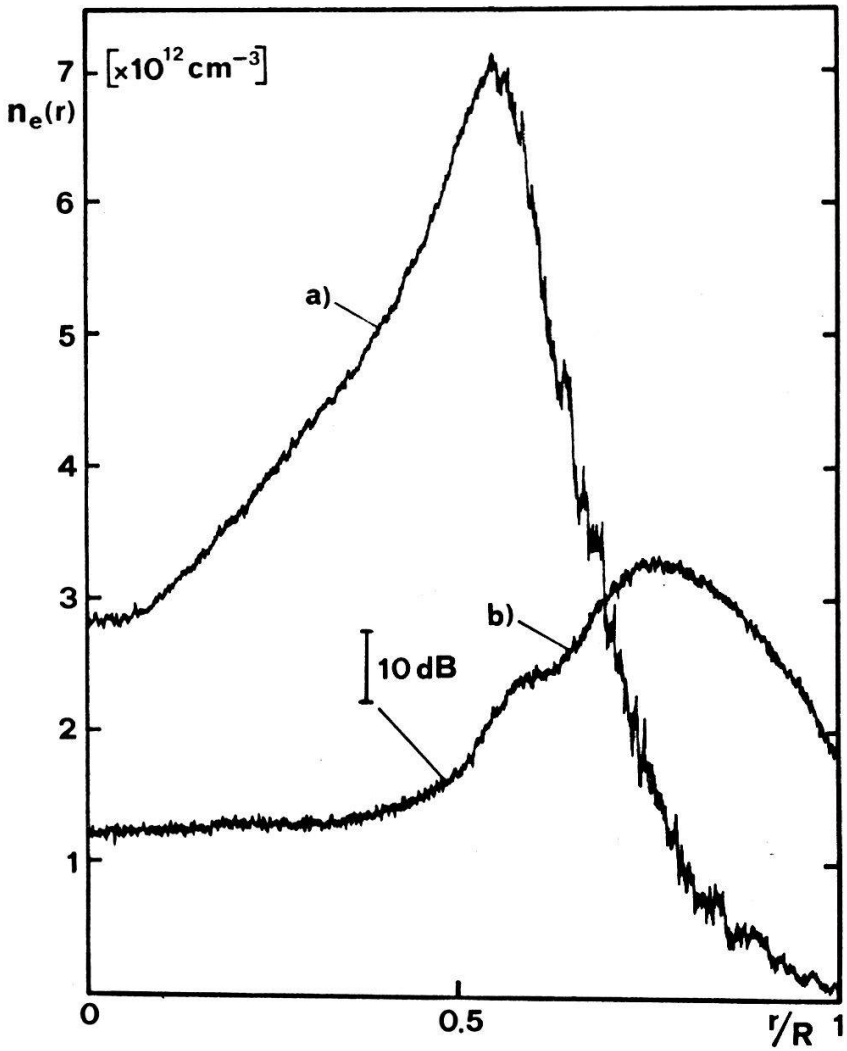

Figure 10
Density profile (a) and the auto power signal of the fluctuations (b).

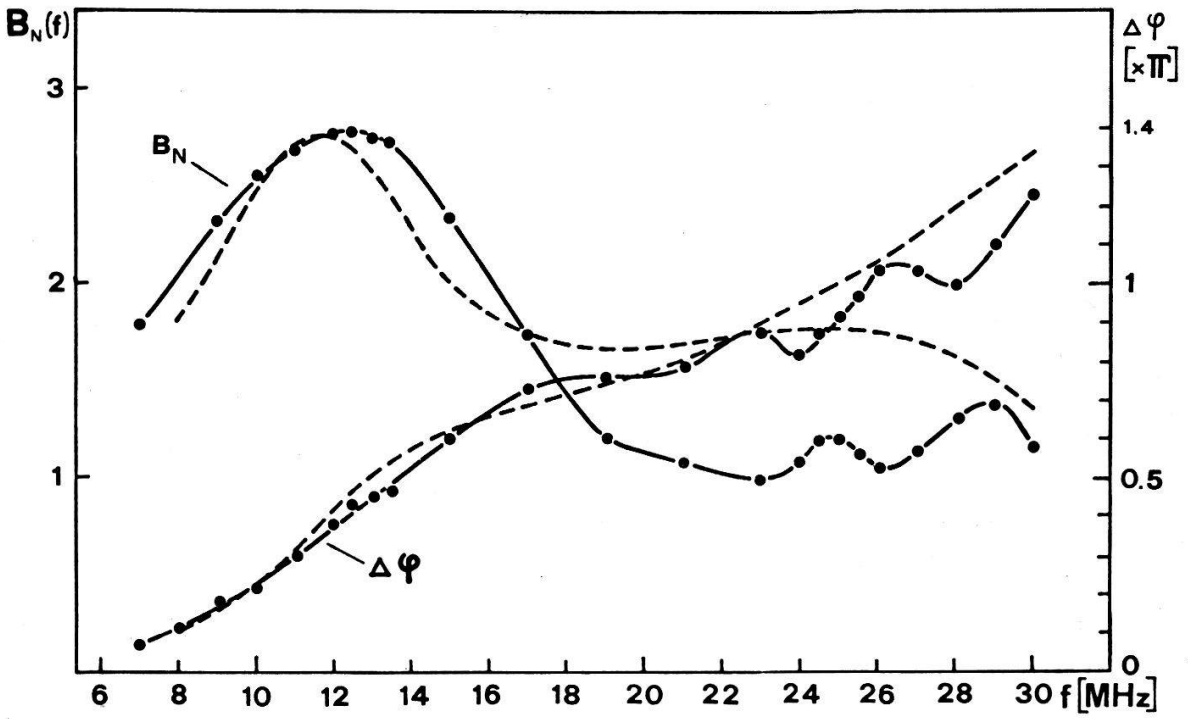

Figure 11
Magnetoacoustic resonance. Normalized amplitude and phase shift. Dots are experiments. Dashed line is computed with the described ν_{eff}.

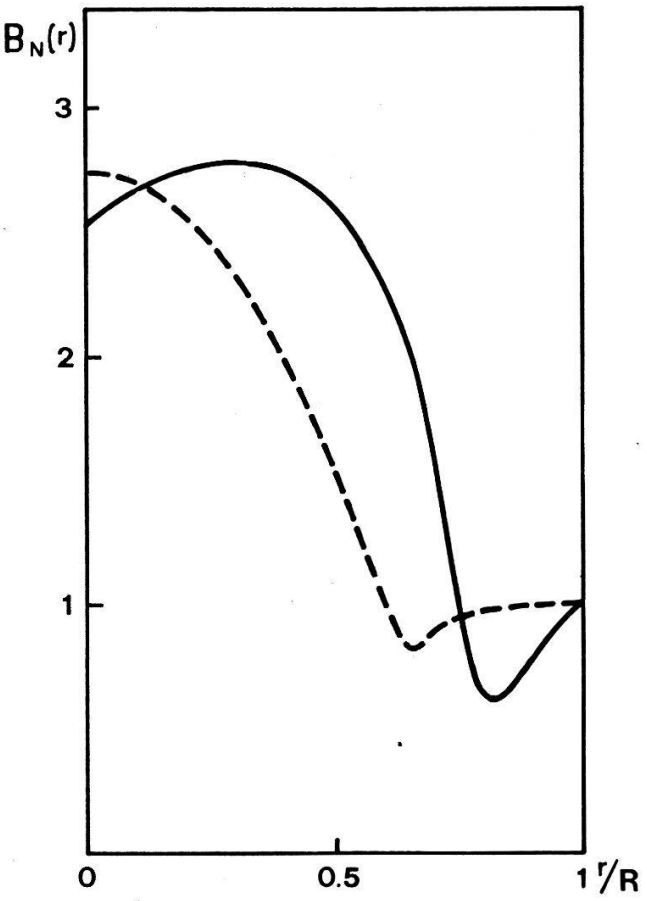

Figure 12
Field distribution in the first radial resonance. Solid line is the experiment. Dashed line is computed with the described ν_{eff}.

collisions in the calculation that depend on the radius and follows the fluctuation energy (b in Fig. 10). The factor of enhancement is equal to 1 on the axis and increases up to 50 at about $r/R = 0.8$.

The result of this calculation is given in Fig. 11 together with the same experimental points of Fig. 9 but in linear scale. Here also the phaseshift is given. Near the first radial resonance – where the phase shift becomes $\pi/2$ – the agreement appears to be very good. At higher frequencies there is still a discrepancy but only within a factor of two.

Beside this the radial dependent enhancement of collisions in the calculation describes details in the field distribution remarkably well. With a density and fluctuation profile as shown in Fig. 10 the field distribution always shows a decrease of amplitude near the boundary. Such a field distribution is shown in Fig. 12. This dip appears in the calculation if the collisions are enhanced at the boundary as described.

Another effect is observed here namely a slight asymmetry of the cylinder. This has been verified experimentally and it was found that a small asymmetry in the density profile is responsible for the shift of the centre line but the amplification is only slightly affected.

V. Conclusion

The amplification in the magnetoacoustic resonance is much smaller than predicted by cold plasma theory even if the inhomogeneity is taken into account. A considerable amount of collision enhancement ($\nu_{\text{eff}} \approx 50\, \nu_{\text{coll}}$) is necessary to explain the observed damping. A justification for this ν_{eff} are the observed fluctuations.

REFERENCES

[1] H. Alfven, *Cosmical Electrodynamics*, Oxford A.T., Clarendon Press 1950.
[2] A. R. Jacobson, C. J. Buchenauer, J. N. Downing and K. S. Thomas, Phys. Rev. Lett. *37* (1976), 897.
[3] T. H. Stix, Bull. Am. Phys. Soc. *21* (1976), 1134.
[4] V. V. Buzankin, V. A. Vershov, N. V. Ivanov, I. A. Kovan, V. A. Krupin, I. A. Popov, I. B. Semenov, and Y. V. Sokolov, Nuclear Fusion Supplement 1977, Vol. III, IAEA-CN-35/Glo.
[5] T. F. R. Group, Nuclear Fusion Supplement 1977, Vol. III, IAEA-CN-35/G8.
[6] B. Hoegger, K. Appert, K. Faessler, L. Krlin and H. Schneider, Helvetica Physica Acta *44* (1971), 321.
[7] H. P. Elmiger, B. G. Vaucher, H. Schneider and J. Vaclavik, Plasma Physics *20* (1978), 921.
[8] M. Kraemer, Plasma Physics *17* (1975), 373.
[9] Y. Sayasov, Helvetica Physica Acta *52* (1979), 171.
[10] J. Musil and F. Zacek, Plasma Physics *16* (1974), 735.
[11] M. A. Heald and C. B. Wharton, *Plasma Diagnostics with Microwaves*, John Wiley Inc., New York 1971.
[12] B. Hoegger and A. Bulliard, Rev. Sci. Instr., to be published.
[13] T. M. Tran, Internal Report, Physics Dept., University of Fribourg, Switzerland, PL-FR 124 (1979).
[14] Ch. Ritz, Internal Report, Physics, Dept., University of Fribourg, Switzerland, PL-FR 127 (1980).
[15] C. R. Skipping, M. E. Oakes and H. Schlueter, Phys. Fluids *12* (1969), 1886.
[16] V. S. Vojtsenya, A. Y. Voloshko, V. M. Zalkind, S. I. Solodovchenko, V. P. Tarasenko and A. F. Stan, Nuclear Fusion *17* (1977), 651.